environmental and earth sciences proceedings

MDPI

Proceeding Paper

The Study of the Urban Heat Island Effect in Cyprus for the Period 2013–2023 by Using Google Earth Engine †

Charalampos Soteriades [1,*], Silas Michaelides [2] and Diofantos Hadjimitsis [1,2]

[1] Department of Civil Engineering and Geomatics, Cyprus University of Technology, Limassol 3036, Cyprus; d.hadjimitsis@cut.ac.cy
[2] Eratosthenes Centre of Excellence, Limassol 3012, Cyprus; silas.michaelides@eratosthenes.org.cy
* Correspondence: sodiriades@cytanet.com.cy
† Presented at the 17th International Conference on Meteorology, Climatology, and Atmospheric Physics—COMECAP 2025, Nicosia, Cyprus, 29 September–1 October 2025.

Abstract

Urbanization in Cyprus has accelerated significantly over the past 35 years, driven by population growth, infrastructure development, and the expansion of urban centres. This rapid urban transformation has contributed to notable changes in the local climate, primarily through the intensification of the Urban Heat Island (*UHI*) effect—a phenomenon where urban areas experience significantly higher temperatures than surrounding rural regions. As global climate change continues to influence regional weather patterns, understanding and mitigating local climatic variations such as *UHI* becomes increasingly critical for sustainable development and public health. In Cyprus, the cities of Nicosia, Limassol, Larnaca, and Paphos have witnessed considerable land use changes, with a growing contrast between densely built urban cores and less developed surrounding areas. This contrast results in uneven energy absorption, reduced vegetation cover, and altered surface temperatures, further exacerbating the effects of climate change at the local level.

Keywords: remote sensing; urban heat island; vegetation cover; urban areas; correlation

Academic Editor: Panagiotis T. Nastos

Published: 12 November 2025

Citation: Soteriades, C.; Michaelides, S.; Hadjimitsis, D. The Study of the Urban Heat Island Effect in Cyprus for the Period 2013–2023 by Using Google Earth Engine. *Environ. Earth Sci. Proc.* **2025**, *35*, 80. https://doi.org/10.3390/eesp2025035080

1. Introduction

In recent decades, urbanization has emerged as a dominant global trend, with more than 50% of the world's population currently living in cities—a figure projected to increase significantly by 2050, particularly in developing regions. This rapid urban expansion, while often associated with economic growth and improved infrastructure, also contributes to a host of environmental challenges. One of the most critical among these is its influence on the local and regional climate.

Urban development alters the natural landscape, replacing vegetated areas with impervious surfaces such as asphalt, concrete, and dense building materials. These changes in land use and land cover (LULC) affect the energy balance of the Earth's surface by modifying surface albedo, increasing heat storage, and reducing evapotranspiration [1,2]. As a result, urban areas tend to exhibit elevated air and surface temperatures compared to their rural surroundings—a phenomenon widely known as the Urban Heat Island (*UHI*) effect [3,4].

The *UHI* effect is not only a localized warming pattern but also an indicator of broader climate-related impacts, including increased energy consumption for cooling, elevated greenhouse gas emissions, deteriorated air quality, and public health concerns such as heat stress. These issues are becoming increasingly prominent as global climate change intensifies, compounding the risks and vulnerabilities faced by urban populations.

Cyprus, a Mediterranean island experiencing both significant urbanization and increasing climate variability, presents a relevant case study for investigating the *UHI* phenomenon [5,6]. Over the past 35 years, major urban centres such as Nicosia, Limassol, Larnaca, and Paphos have undergone rapid development, leading to substantial transformations in their LULC patterns. The resulting climatic differentiation between urban and surrounding rural zones highlights the urgency of monitoring and understanding the *UHI* effect within the specific context of Cyprus [7].

This study aims to assess the spatial and temporal dynamics of the Urban Heat Island effect across the main cities of Cyprus using Remote Sensing techniques via Google Earth Engine (GEE) [8]. By integrating satellite-derived indices and spatial data analytics, we explore the relationship between urban land cover characteristics—particularly vegetation cover and built-up density—and surface temperature anomalies. The insights derived from this research can inform local policymakers and urban planners, helping to develop targeted climate adaptation strategies and sustainable land use policies that mitigate the impacts of urban heat in Cyprus.

The highest temperatures with the corresponding dates have been taken from the Cyprus Department of Meteorology for the years 2016–2022, for the four major cities of Cyprus. Cyprus is an island situated in the eastern Mediterranean Sea, and is part of the wider area of the East Mediterranean, Middle East, and North Africa (EMMENA) region [9]. With a total area of 9254 km^2, the island has a semi-arid climate that experiences frequent droughts. Furthermore, it is noted that Cyprus's climate exhibits spatiotemporal behaviour due to the various topographic features brought about by the island's hilly terrain. Cyprus experiences typical Mediterranean summers that are hot and dry and mild winters that are rainy. Urbanization, changes in land use, and alteration of natural land cover are the main drivers of *UHI* in Cyprus. Natural vegetation is replaced by impermeable surfaces like concrete and asphalt when cities grow, which results in less evaporative cooling and more heat absorption. The fast growth of Cyprus's cities (Paphos, Limassol, Nicosia, Larnaca) has led to changes in land use and increased urban congestion.

2. Materials and Methods

NASA's Landsat-8 satellite data covers the years 2013 through 2023, acquired for this investigation through Google Earth Engine [10]. The imagery was collected annually between May 1st and September 30th, with an emphasis on the warmest months to capture the summer-time phenomena known as the Urban Heat Island (*UHI*). To assure data accuracy, clouds and cloud shadows were masked using the Landsat Surface Reflectance Quality Assessment (QA) band. Clouds and cloud shadows can drastically alter temperature readings and spectral index computations. Before processing, scaling factors were applied to the Landsat-8 images to guarantee the data's accuracy and comparability. For both optical and thermal bands, these scaling factors translate digital numbers (DN) to physical units.

The scale factors applied were 0.0000275 and −0.2 for optical bands and 0.00341802 and 149.0 for thermal bands. Using Google Earth Engine, Landsat 8 images were retrieved for the four major cities of Cyprus.

The integration of vegetation indices such as *NDVI* and *FVC* allows for a robust quantification of vegetation health and its role in moderating thermal extremes [11]. Coupled with urban thermal indicators like *UTFVI*, these metrics provide a comprehensive assessment of the thermal heterogeneity in urban environments, offering valuable insight for urban heat mitigation strategies [12,13].

Thermal and vegetation indices were computed using data from the Landsat-8 satellite. In order to evaluate vegetation cover and to conduct a correlation analysis between the

intensification of *UHI* and vegetation in urban and rural areas, the Normalized Difference Vegetation Index (*NDVI*), which is denoted in Equation (1), and the Fraction of Vegetation Cover (*FVC*), which is denoted in Equation (2), were employed.

NDVI is a popular vegetation index that is used to determine the health and growth of vegetation in an area of interest:

$$NDVI = \frac{(NIR - Red)}{(NIR + Red)} \quad (1)$$

where *NIR* is the Near-Infrared band and Red is the Red band of Landsat-8.

FVC is a proxy of *NDVI,* which is important to determine the vegetation cover in a study area:

$$FVC = \left(\frac{NVDI - NVDI_{min}}{NVDI_{max} - NDVI_{min}} \right) \quad (2)$$

where *NDVI* is the *NDVI* at the current pixel, $NDVI_{min}$ is the minimum observed *NDVI* value in an area of interest, and $NDVI_{max}$ is the maximum observed *NDVI* value in an area of interest.

Furthermore, to evaluate surface temperature changes and quantify the intensity of *UHI*, which is defined in Equation (3), thermal indices such as Emissivity (*EM*) and Land Surface Temperature (*LST*), defined in Equations (4) and (5), respectively, were calculated. Moreover, another index was calculated for the assessment, the Urban Thermal Field Variance Index (*UTFVI*), which is defined in Equation (6). These indices offer vital insights into urban microclimates and inform urban planning strategies.

$$UHI = \frac{LST - LST_{mean}}{LST_{std}} \quad (3)$$

where LST_{mean} is the mean *LST*, and LST_{std} is the standard deviation of *LST* of the study area.

Emissivity is defined as the ratio of energy radiated from a material's surface to that radiated from a perfect emitter. Satellite *EM* is a proxy of the vegetation cover in an area:

$$EM = 0.004 \times FVC + 0.986 \quad (4)$$

where *FVC* is calculated from Equation (2).

LST is the satellite-based Land Surface Temperature, defined as follows:

$$LST = \frac{T_b}{1 + \left(0.00115 \times \frac{T_b}{0.48359547432}\right) \times \log(EM)} - 273.15 \quad (5)$$

where T_b represents the temperature acquired from the thermal band of Landsat-8 and *EM* is the emissivity calculated from Equation (3).

UTFVI is often used to assess the thermal quality of urban areas,

$$UTFVI = \frac{LST - LST_{mean}}{LST} \quad (6)$$

where *LSTmean* is the mean *LST* and *LST* is calculated from Equation (5).

Moreover, air temperature measurements at 1.2 m were collected from the archives of the Department of Meteorology of Cyprus in the major cities of Cyprus (Table 1). These measurements were collected to investigate temperature fluctuations during the summer period, providing valuable data for understanding urban heat island effects and assisting in the formulation of strategies for climate change resilience and adaptation in urban areas.

Table 1. Maximum temperature (°C) recorded in the four major cities of Cyprus.

Year	Pafos		Limassol		Nicosia		Larnaca	
	Temperature	Date	Temperature	Date	Temperature	Date	Temperature	Date
2023	38.1	24/7	38.2	24/7	45.3	14/8	40.4	24/7
2022	35.6	22/6	35.1	19/7	42	28/7	36.1	18/7
2021	37.3	28/7	38.3	16/7	44.3	4/8	39.2	6/8
2020	35.2	22/8	38.5	31/8	45.3	4/9	39.1	31/8
2019	33	8/8	36.6	3/6	42.1	25/6	36.4	21/7
2018	33.5	5/7	38.3	23/7	41.7	14/8	37.8	6/7
2017	41.6	1/7	41.4	2/7	44.6	2/7	39.9	1/7
2016	37.8	17/6	39.1	20/6	42.2	23/6	38	20/6
2015	35	3/8	41.3	4/8	42.5	3/8	39.6	3/8
2014	33.8	24/8	37.5	24/8	41.3	28/6	38	28/6
2013	36	19/6	40.5	17/6	39.8	15/8	37	17/8
2012	35.6	18/7	39.5	6/8	43.6	17/7	38.5	7/8
2011	34.8	27/7	38	10/6	41.3	9/8	37.1	17/7
2010	35.2	17/6	39.6	18/8	45.6	1/8	38.6	2/8

In climate studies, temperature generally refers to two key aspects:

- Surface Temperature: This refers to the temperature of the Earth's surface, which can be measured using remote sensing technologies like satellites. It reflects how much heat is being absorbed or emitted by the ground, buildings, roads, and other surfaces in an urban area. Urban surfaces, such as asphalt or concrete, tend to absorb and retain more heat compared to natural land cover like vegetation or soil. This leads to higher surface temperatures in urban areas, contributing to the Urban Heat Island effect.
- Air Temperature: This refers to the temperature of the atmosphere at a particular height above ground (often at 1.5 m). It measures the warmth of the air that people experience and can be influenced by various factors such as wind, humidity, and the underlying surface. In cities, air temperatures are typically higher than in rural areas due to the heat retained by buildings and roads and the lack of vegetation to cool the air through evapotranspiration.

Both surface and air temperatures are crucial when studying the Urban Heat Island effect because they help explain the extent to which urbanization contributes to local temperature variations.

The linear relationships between the variables are assessed via Pearson correlation as defined by Equation (7). When its value is near +1, a strong positive linear relationship is indicated; when the value is near -1, a strong negative linear relationship is indicated. When the value is zero, a little to no linear relationship is indicated. On the other hand, monotonic relationships between the variables are measured by Spearman correlation, which is calculated by Equation (8). As long as there is a consistent general trend, the statistical methodology is unaffected by a constant (linear) increase or decrease. When the value is approaching +1, a positive monotonic trend is exhibited; when the value is approaching -1, a negative monotonic trend is exhibited. When the value is close to zero, a slight to no monotonic relationship is suggested.

Pearson's correlation coefficient is defined by the following:

$$r = \frac{\sum(x_i - \overline{x})(y_i - \overline{y})}{\sqrt{\sum(x_i - \overline{x})^2 \sum(y_i - \overline{y})^2}} \quad (7)$$

where x_i are the values of the x-variable in a sample, $\overline{x}$ is the mean value of the x-variable; y_i are the values of the y-variable in the sample and $\overline{y}$ is the mean value of the y-variable.

Spearman's rank correlation coefficient is defined by the following:

$$\rho = 1 - \frac{6\sum d_i^2}{n(n^2-1)} \quad (8)$$

where d_i is the observation differences between the two ranks, and n is the number of observations.

3. Results

The highest temperatures ever recorded in the four significant cities (i.e., Paphos, Limassol, Nicosia, and Larnaca) are shown in Figure 1 for the decade from 2013 to 2023. The cities with the highest average maximum temperatures are Nicosia, Limassol, and Paphos. Over the course of the observation period, Larnaca exhibits the coolest maximums. All four cities exhibit a general upward trend in maximum temperatures, despite some annual fluctuations. When comparing the maximum temperatures in 2013—which were roughly 20 °C—to 2023—when they are closer to 30 °C—this trend becomes especially evident. Moreover, the warmest day in Cyprus during 2013 to 2023 was recorded in Nicosia, with more than 40 °C.

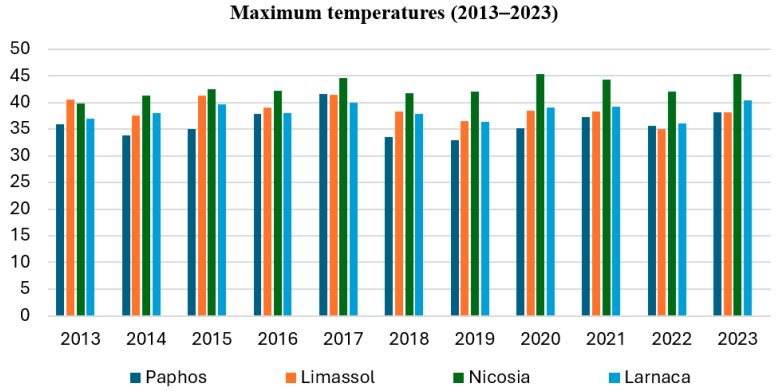

Figure 1. Maximum temperatures (°C) in Cyprus' four major cities, from 2013 to 2023.

Based on the temporal distributions in Figure 2, referring to the four cities' rural areas, it is easily recognized that Limassol's rural area faces less intense *UHI* phenomena. On the other hand, Paphos and Larnaca are facing some fluctuations in such events in their rural areas, while both during 2023 reached the low levels of *UHI*, similar to Limassol. Nicosia's rural areas are facing the most intense *UHI* phenomena during the decade 2023.

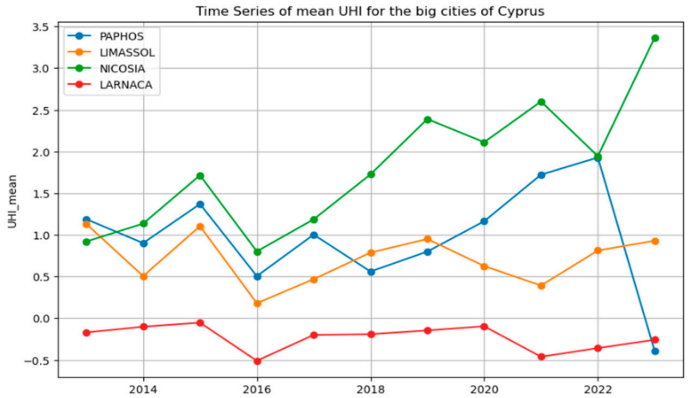

Figure 2. Time series of UHI for the four major cities' rural areas of Cyprus during 2013–2023.

Negative Pearson's and Spearman's correlations (shown in Table 2) imply that when the vegetation cover (*FVC*) both in rural areas of Cyprus and major cities' centres decreases,

intense Urban Heat Island phenomena are noted. The same is true for the relationship between vegetation cover and Urban Thermal Field Variance Index (*UTFVI*).

Table 2. Pearson and Spearman correlation coefficient for the correlation between *FVC* and *UHI*, and the correlation between *FVC* and *UTFVI* at the major cities' centres and surrounding rural areas.

	Pearson		**Spearman**	
	FVC-UHI	***FVC-UTFVI***	***FVC-UHI***	***FVC-UTFVI***
Rural areas	−0.446	−0.382	−0.391	−0.372
City centre	−0.287	−0.214	−0.581	−0.214

4. Concluding Remarks

In this work, a correlation analysis using Spearman and Pearson coefficients was conducted to realize the relations between vegetation coverage in cities and rural areas of Cyprus with the phenomenon of *UHI* and the *UTFVI*. This analysis showed that the loss of green spaces in urban centres and the urbanization of rural areas over the years are leading to intense *UHI* events in Cyprus. Furthermore, an intensification of *UTFVI* is also observed.

Author Contributions: Conceptualization, C.S. and D.H.; methodology, C.S. and D.H.; software, C.S.; validation, C.S. and S.M.; formal analysis, C.S.; investigation, C.S. and S.M.; data curation, C.S.; writing—original draft preparation, C.S.; writing—review and editing, C.S. and S.M.; visualization, C.S.; supervision, D.H.; project administration, D.H.; funding acquisition, D.H. All authors have read and agreed to the published version of the manuscript.

Funding: The authors acknowledge the 'EXCELSIOR': ERATOSTHENES: Excellence Research Centre for Earth Surveillance and Space-Based Monitoring of the Environment H2020 Widespread Teaming project (www.excelsior2020.eu, accessed on 1 September 2025). The 'EXCELSIOR' project has received funding from the European Union's Horizon 2020 research and innovation programme under Grant Agreement No 857510, from the Government of the Republic of Cyprus through the Directorate General for the European Programmes, Coordination and Development and the Cyprus University of Technology.

Institutional Review Board Statement: Not applicable.

Informed Consent Statement: Not applicable.

Data Availability Statement: Data are available from the Department of Meteorology, Nikis 28, 1086 Nicosia, Cyprus.

Conflicts of Interest: The authors declare no conflict of interest.

References

1. Gluch, R.; Quattrochi, D.A.; Luvall, J.C. A multi-scale approach to urban thermal analysis. *Remote Sens. Environ.* **2006**, *104*, 123–132. [CrossRef]
2. Hadjimitsis, D.G.; Retalis, A.; Michaelides, S.; Tymvios, F.; Paronis, D.; Themistocleous, K.; Agapiou, A. Satellite and ground measurements for studying the Urban Heat Island Effect in Cyprus. In *Remote Sensing of Environment-Integrated Approaches, Chapter 1*; Hadjimitsis, D., Ed.; InTech: London, UK, 2013.
3. Zhang, Y.; Cheng, J. Spatio-temporal analysis of urban heat island using multisource remote sensing data: A case study in Hangzhou, China. *IEEE J. Sel. Top. Appl. Earth Obs. Remote Sens.* **2019**, *12*, 3317–3326. [CrossRef]
4. Kaplan, G. Evaluating the roles of green and built-up areas in reducing a surface urban heat island using remote sensing data. *Urbani Izziv* **2019**, *2*, 105–112. [CrossRef]
5. Cecinati, F.; Amitrano, D.; Leoncio, L.B.; Walugendo, E.; Guida, R.; Iervolino, P.; Natarajan, S. Exploitation of ESA and NASA heritage remote sensing data for monitoring the heat island evolution in Chennai with the Google Earth Engine. In Proceedings of the IGARSS 2019–2019 IEEE International Geoscience and Remote Sensing Symposium, Yokohama, Japan, 28 July–2 August 2019; pp. 6328–6331.

6. Liebowitz, A.; Sebastian, E.; Yanos, C.; Bilik, M.; Blake, R.; Norouzi, H. Urban Heat Islands and Remote Sensing: Characterizing Land Surface Temperature at the Neighborhood Scale. In Proceedings of the IGARSS 2020–2020 IEEE International Geoscience and Remote Sensing Symposium, Waikoloa, HI, USA, 26 September–2 October 2020; pp. 4407–4409.
7. Li, N.; Li, X. The Impact of Building Thermal Anisotropy on Surface Urban Heat Island Intensity Estimation: An Observational Case Study in Beijing. *IEEE Geosci. Remote Sens. Lett.* **2020**, *17*, 2030–2034. [CrossRef]
8. Weng, Q.; Rajasekar, U.; Hu, X. Modeling Urban Heat Islands and their relationship with impervious surface and vegetation abundance by using ASTER images. *IEEE Trans. Geosci. Remote Sens.* **2011**, *49*, 4080–4089. [CrossRef]
9. Eliades, M.; Michaelides, S.; Evagorou, E.; Fotiou, K.; Fragkos, K.; Leventis, G.; Theocharidis, C.; Panagiotou, C.F.; Mavrovouniotis, M.; Neophytides, S.; et al. Earth Observation in the EMMENA region: Scoping review of current applications and knowledge gaps. *Remote Sens.* **2023**, *15*, 4202. [CrossRef]
10. Gorelick, N.; Hancher, M.; Dixon, M.; Ilyushchenko, S.; Thau, D.; Moore, R. Google Earth Engine: Planetary-scale geospatial analysis for everyone. *Remote Sens. Environ.* **2017**, *202*, 18–27. [CrossRef]
11. Oke, T.R. The energetic basis of the urban heat island. *Q. J. R. Meteorol. Soc.* **1982**, *108*, 1–24. [CrossRef]
12. Voogt, B.; Oke, T. Thermal remote sensing of urban climates. *Remote Sens. Environ.* **2003**, *86*, 370–384. [CrossRef]
13. Imhoff, M.L.; Zhang, P.; Wolfe, R.E.; Bounoua, L. Remote sensing of the urban heat island effect across biomes in the continental USA. *Remote Sens. Environ.* **2010**, *114*, 504–513. [CrossRef]